Lawrence Berkeley National Laboratory

Title
Canopy and physiological controls of GPP during drought and heat wave

Permalink
https://escholarship.org/uc/item/9sz3n0d2

Journal
Geophysical Research Letters, 43(7)

ISSN
0094-8276

Authors
Zhang, Yao
Xiao, Xiangming
Zhou, Sha
et al.

Publication Date
2016-04-16

DOI
10.1002/2016gl068501

Peer reviewed

Canopy and physiological controls of GPP during drought and heat wave

Yao Zhang[1], Xiangming Xiao[1,2], Sha Zhou[3,4], Philippe Ciais[5], Heather McCarthy[6], and Yiqi Luo[6]

[1] Department of Microbiology and Plant Biology, Center for Spatial Analysis, University of Oklahoma, Norman, Oklahoma, USA, [2] Institute of Biodiversity Science, Fudan University, Shanghai, China, [3] State Key Laboratory of Hydroscience and Engineering, Department of Hydraulic Engineering, Tsinghua University, Beijing, China, [4] Department of Civil and Environmental Engineering, Princeton University, Princeton, New Jersey, USA, [5] Laboratoire des Sciences du Climat et de l'Environnement, CEA CNRS UVSQ, Gif-sur-Yvette, France, [6] Department of Microbiology and Plant Biology, University of Oklahoma, Norman, Oklahoma, USA

Correspondence to: X. Xiao, xiangming.xiao@ou.edu

Abstract

Vegetation indices (VIs) derived from satellite reflectance measurements are often used as proxies of canopy activity to evaluate the impacts of drought and heat wave on gross primary production (GPP) through production efficiency models. However, GPP is also regulated by physiological processes that cannot be directly detected using reflectance measurements. This study analyzes the co-limitation of canopy and plant physiology (represented by VIs and climate anomalies, respectively) on GPP during the 2003 European summer drought and heat wave for 15 Euroflux sites. During the entire drought period, spatial pattern of GPP anomalies can be quantified by relative changes in VIs. We also find that GPP sensitivity to relative canopy changes is higher for nonforest ecosystems (1.81 ± 0.32%GPP/%enhanced vegetation index), while GPP sensitivity to physiological changes is higher for forest ecosystems ($-0.18 \pm 0.05\,\mathrm{g\,C\,m^{-2}\,d^{-1}}$/hPa). A conceptual model is further built to better illustrate the canopy and physiological controls on GPP during drought periods.

1 Introduction

Both drought frequency and intensity are predicted to increase along with global warming [*Dai*, 2012; *Easterling et al.*, 2000], which can alter the carbon cycle through inhibiting photosynthesis [*Flexas and Medrano*, 2002], increasing mortality rate [*Allen et al.*, 2010; *Peng et al.*, 2011], and affecting ecosystem structure [*Saatchi et al.*, 2013]. The decrease of net primary production caused by drought was estimated to be 0.55 Pg C globally for the first decade in the 21st century [*Zhao and Running*, 2010]. The most direct effect of drought came from the declined gross primary production (GPP) [*Ciais et al.*, 2005]. Many approaches have been proposed to estimate GPP at regional or global scale: (1) process-based dynamic global vegetation models [*Arora et al.*, 2013; *Sitch et al.*, 2008], (2) remote sensing-based production

efficiency models (PEMs) [*Zhao and Running*, 2010], and (3) eddy flux-based data-driven models [*Beer et al.*, 2010; *Jung et al.*, 2011]. *Vetter et al*. [2008] compared the predictions of these models for GPP and net ecosystem CO2 exchange anomalies during the 2003 European drought and heat wave. But the results from seven models were divergent, with estimates of drought-induced GPP decline ranging from −0.02 to −0.27 Pg C. A clear difference has also been found between the eddy flux-based data-driven models which show little interannual variability (IAV) and the process-based models which exhibit larger IAV [*Anav et al.*, 2015]. Since drought is one of the most important factors which causes the IAV of GPP [*Zscheischler et al.*, 2014], it is crucial to improve the accuracy of GPP estimation during drought and heat wave to better understand the ecosystem responses under future climate.

Drought and heat wave have two direct impacts on plant photosynthesis [*der Molen et al.*, 2011]. The first impact is the physiological response to water deficit and high temperature, including the reduction in enzyme activity, and stomatal conductance to prevent water loss [*Flexas and Medrano*, 2002; *Hetherington and Woodward*, 2003; *Reichstein et al.*, 2002]. These effects have been often related to temperature, vapor pressure deficit [*Farquhar et al.*, 1980], and soil moisture deficit [*Baldocchi et al.*, 2004]. The second impact is the changes of vegetation canopy in response to drought, which includes leaf withering and senescence. The canopy changes can be represented by the decrease of leaf area index (LAI) and observed by satellites [*Zhang et al.*, 2013]. These two processes also take effects at different time scales: the physiological processes respond at the scale of minutes to days, while the vegetation canopy changes occur at a scale of days to weeks.

Satellite-based PEMs differ in their approaches to quantify physiological and canopy responses to drought and heat. Some PEMs use vapor pressure deficit (VPD)-related scalars, e.g., MODIS PSN (Moderate Resolution Imaging Spectroradiometer Photosynthesis) [*Running et al.*, 2004] and carbon flux model [*Turner et al.*, 2006]. However, GPP responses to VPD and temperature are different among ecosystems, even species [*Blackman and Brodribb*, 2009]. For example, both the stomata characteristics (size and density) and intrinsic water use efficiency (A/gs, carbon assimilation rate divided by stomatal conductance) differ among individual vegetation types [*Hetherington and Woodward*, 2003]. Therefore, using universal parameters to qualify these limitations will introduce biases. Some PEMs use transformed vegetation indices (VIs) to account for water stress, including VPM (vegetation photosynthesis model) [*Xiao et al.*, 2004b], vegetation photosynthesis and respiration model [*Mahadevan et al.*, 2008], and modified temperature and greeness model [*Sims et al.*, 2014]. However, when the vegetation canopy responds to prolonged drought and heat, different ecosystems have different spectral sensitivities to water stress (SSWS), i.e., the changes in canopy characteristics which can be captured by satellite under water stress [*Sims et al.*, 2014]. Trees with deeper roots are

more resistant to decreased soil water and have low SWSS. By contrast, SWSS are generally higher for grassland and shrubland. In addition, there may be a time lag between leaf senescence and GPP decline for most plants, which makes simulating GPP under drought even more difficult [*Frank et al.*, 2015]. *Dong et al*. [2015] suggested that remote sensing data-driven models that do not include water limitation factors performed much worse during drought periods. However, even for the models discussed above which consider water stress, their performances are not satisfied [*Liu et al.*, 2015; *Schaefer et al.*, 2012]. The major problem is the oversensitivity of VPD-related water stress and undersensitivity of VIs-related water stress. Recent studies also highlight the complexity of water stress limitation on GPP and light use efficiency [*Yuan et al.*, 2014; *Zhang et al.*, 2015b]. Improving PEMs performance is critical to better diagnose the effects of droughts and heat waves on GPP.

The 2003 summer climate anomaly in Europe is suitable to investigate physiological and canopy controls on regional GPP, because of the relatively high density of flux tower sites, different ecosystems affected, and the large spatial extent of the drought [*Schar et al.*, 2004]. In this paper, we address two specific questions: (1) Are satellite-retrieved VIs sufficient to quantify the spatial differences in GPP anomalies across different ecosystems? (2) Are satellite-retrieved VIs able to track the temporal GPP anomalies at each flux tower site?

2 Materials and Methods

2.1 Data

The data used in this study include remotely sensed vegetation indices (VIs) and land surface temperature (LST), as well as vapor pressure deficit (VPD) and GPP measurements from the in situ flux tower records. VIs and LST for each site are derived from MODIS (MOD09A1 and MOD11A2). Even during drought period, there exists atmospheric contamination on data quality [*Zhang et al.*, 2015a]. In order to eliminate these corrupted observations, a data quality check and gap-filling algorithm was applied to these variables (Figure S1 in the supporting information). The eddy flux data are from 15 flux tower sites in Europe, all of which experienced a decline of GPP during the 2003 drought and heat wave period (Figures 1a–1c and Table S1). For more information about the data usage and processing, please refer to the supporting information.
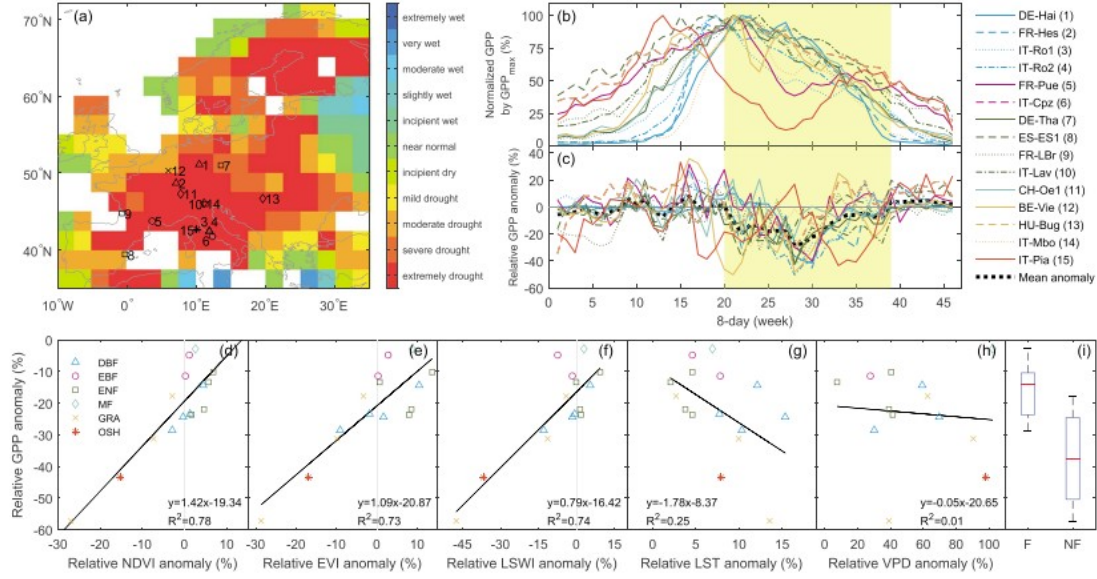
Figure 1. (a) Location of the flux tower sites used in this study and the averaged drought intensity from June to October in 2003. The drought intensity was indicated by the Palmer Drought Severity Index (PDSI) averaged over the drought period. PDSI data were downloaded from the National Center for Atmospheric Research Climate & Global Dynamics (NCAR-CGD) website (http://www.cgd.ucar.edu/cas/catalog/climind/pdsi.html) [*Dai*, 2012]. Site ID in the map can be interpreted using the legend for Figure 1b. (b) Seasonal GPP normalized by maximum GPP for normal years. (c) GPP relative anomalies for 2003 for 15 flux tower sites. Different colors represent different vegetation types, using the same colors as Figure 1d. The black dashed line represents the average anomaly of all the 15 sites. (d–h) Relationship of averaged relative anomalies for the entire drought and heat wave period ($\overline{\sigma_7}$) between GPP and vegetation indices (EVI, NDVI, and LSWI), land surface temperature (LST), and vapor pressure deficit (VPD). (i) GPP decrease for forest (F) and nonforest (NF) in relative anomaly.

2.2 Method

GPP can be calculated based on a function of a maximum potential value, GPP_{max}, reduced by both canopy control (CC) and physiological control (PC)

$$GPP = GPP_{max} \times f(CC, PC) \quad (1)$$

For each specific stable ecosystem, the GPP_{max} for a specific period can be regarded as a constant. The canopy control is related to three different characteristics of vegetation canopy: (1) leaf area or canopy coverage, (2) canopy pigments such as chlorophyll content, and (3) canopy water content [*Xiao et al.*, 2005]. The physiological control is the environmental stress on carbon fixation process through stomatal conductance, enzyme activity, etc. We hypothesize that canopy control and physiological control are independent because they respond at different time scales. Therefore, the differential form of GPP with respect to these two controls is as follows:

$$dGPP = GPP_{max} \times \left(\frac{\partial GPP}{\partial CC} dCC + \frac{\partial GPP}{\partial PC} dPC \right) \quad (2)$$

The relative change in GPP can be calculated as

$$\frac{dGPP}{\overline{GPP}} = GPP_{max} \times \left(\frac{\partial GPP/\overline{GPP}}{\partial CC/\overline{PC}} \frac{dCC}{\overline{PC}} + \frac{\partial GPP/\overline{GPP}}{\partial PC/\overline{PC}} \frac{dPC}{\overline{PC}} \right) \quad (3)$$

If we change the form of equations 2 and 3 and replace $GPP_{max} \times \frac{\partial GPP}{\partial CC}$ and $GPP_{max} \times \frac{\partial GPP}{\partial PC}$ with Φ_{CC} and Φ_{PC} and $GPP_{max} \times \frac{\partial GPP/\overline{GPP}}{\partial CC/\overline{CC}}$ and $GPP_{max} \times \frac{\partial GPP/\overline{GPP}}{\partial PC/\overline{PC}}$ with φ_{CC} and φ_{PC}, equations 2 and 3 are rewritten as

$$\Delta GPP = \Phi_{CC} \times \Delta CC + \Phi_{PC} \times \Delta PC \quad (4)$$

$$\delta GPP = \varphi_{CC} \times \delta CC + \varphi_{PC} \times \delta PC \quad (5)$$

Φ_{CC} and Φ_{PC} indicate the sensitivity of GPP to the absolute change (Δ) of canopy and physiological controls, respectively. φ_{CC} and φ_{PC} represent the sensitivity of GPP to the relative change (δ) of canopy and physiological controls, respectively. The absolute anomaly (Δ) and relative anomaly (δ) can be calculated as below:

$$\Delta_\gamma^i = \gamma_i - \overline{\gamma_i} \quad (6)$$

$$\delta_\gamma^i = \frac{\gamma_i - \overline{\gamma_i}}{\overline{\gamma_i}} \quad (7)$$

where γ stands for different variables (e.g., VIs, GPP, and VPD). γ_i and $\overline{\gamma_i}$ represent the ith observation for each 8 day period (hereafter referred to as week) in 2003 and the average value of the variable γ for the corresponding week for normal years, respectively. For each site, the normal years are defined as the years with flux observations, excluding 2003. $\overline{\Delta_\gamma}$ and $\overline{\delta_\gamma}$ denote the anomalies calculated from the entire drought period in 2003 compared to normal years. The drought period is defined as weeks 20 to 39 (2 June to 8 November) in 2003, when the average δ_{GPP} of the 15 flux sites drops below 0 (Figures 1b and 1c).

The two limitations are represented by indicators that can be directly observed. The canopy control (CC) is represented by three VIs, namely, the normalized difference vegetation index (NDVI), the enhanced vegetation index (EVI), and the land surface water index (LSWI). These three VIs are selected because they are related to different properties of the canopy. NDVI is related to the leaf area [*Carlson and Ripley*, 1997], EVI is related to the green leaf [*Zhang et al.*, 2005], and LSWI is related to the water content in the canopy [*Xiao et al.*, 2004a]. The physiological control (PC) is represented by satellite-retrieved LST and VPD from flux tower measurements, both of which are frequently used in PEMs.

Based on absolute and relative anomalies (equations 6 and 7), we investigate the relationship between GPP anomalies and anomalies of VIs, LST, and VPD for the entire drought period across all flux sites ($\overline{\Delta_\gamma}$ and $\overline{\delta_\gamma}$ were used). To explore the respective effects of the physiological and canopy controls during the drought period for each site, we first use VPD as the physiological control and analyze the partial correlation between dependent variable Δ_{GPP} or δ_{GPP} and two corresponding independent variables (Δ_{VIs} or δ_{VIs} and Δ_{VPD} or δ_{VPD}), represented by $\rho_\Delta^{GPP, \gamma}$ or $\rho_\sigma^{GPP, \gamma}$ (γ represents VIs or VPD, with the other controlled), respectively. We also consider a lagged response of VIs

to GPP change with lags of 0 to 5 weeks. Previous studies suggested that lags from weeks to months exist for satellite-retrieved canopy signals and precipitation decline [*Ji and Peters*, 2003; *Wan et al.*, 2004]. LST and VPD, which directly affect enzyme activity and stomatal conductance, respectively, are not analyzed with lags (confirmed by Figures S3 and S4). Based on the partial correlation analysis, we use multivariate regression to fit the GPP data into equations 4 and 5 to get the GPP sensitivity to absolute change (Φ) and relative change (φ) of canopy and physiological controls, respectively. We also take the lag effect on canopy control into consideration; regressions are conducted only for the lags with highest partial correlation in the previous analysis. All these procedures are also conducted using LST instead of VPD as the physiological control.

3 Results

3.1 Sensitivity of GPP Anomalies to Changes in Vegetation Indices and Climate Over the Entire Drought Period

All the 15 sites have negative $\overline{\Delta_{GPP}}$ and $\overline{\delta_{GPP}}$ during the drought period (Table S1). In terms of absolute anomalies, $\overline{\Delta_{GPP}}$ is the largest for grassland (GRA, -377.8 to $-207.3\,\mathrm{g\,C\,m^{-2}}$) and deciduous broadleaf forest (DBF, -321.0 to $-175.0\,\mathrm{g\,C\,m^{-2}}$), followed by evergreen needleleaf forest (ENF, -272.3 to $-93.5\,\mathrm{g\,C\,m^{-2}}$), while three other vegetation types (evergreen broad leaf forest (EBF), mixed forest (MF), and open shrubland (OSH)) have a smaller $\overline{\Delta_{GPP}}$. In terms of relative anomalies, nonforest sites (GRA and OSH) show a much larger $\overline{\delta_{GPP}}$ decline (-57.2% to -17.8%) compared to the forest sites (-28.6% to -2.8%) (Figure 1i and Table S1).

Figures 1d–1h show the relationship between the averaged anomalies of GPP and anomalies of VIs, LST, and VPD during the entire drought period. The canopy responses during the drought period are divergent among sites and show only slight differences when different VIs are used. $\overline{\delta_{VIs}}$ for nonforest are mostly negative, suggesting that the canopy properties are significantly affected during the drought. In contrast, $\overline{\delta_{VIs}}$ for all the forest sites are close to zero, indicating that the canopy optical characteristics merely change. The coefficients of determination between δ_{GPP} and δ_{VIs} are high ($R^2 > 0.73$). The slopes of the regressions are the lowest for LSWI (0.79), suggesting that a small change in GPP corresponds to a larger change in LSWI. The intercepts for the three VIs are similar (~20%). When using absolute anomalies, the correlations between GPP and VIs are much lower (Figure S2).

We also investigated the relationship between the anomalies of GPP and physiological indicators (LST and VPD). During the drought period compared to normal years, LST and VPD increase by 0.49 to 3.71°C and 0.50 to 6.83 hPa, respectively (Table S1). Correlation between $\overline{\delta_{GPP}}$ and $\overline{\delta_{LST}}$ is stronger ($R^2 = 0.25$) than that between $\overline{\delta_{GPP}}$ and $\overline{\delta_{VPD}}$ ($R^2 = 0.01$) or air temperature ($\overline{\delta_{Tair}}$, $R^2 = 0.01$) measured at flux tower sites (Figures 1g, 1h, and S5). Even though all VIs and climate variables respond to drought, only $\overline{\delta_{VIs}}$ show significant correlation with $\overline{\delta_{GPP}}$. This indicates that the spatial difference, i.e., from site

to site, of the GPP decline due to drought and heat wave can be partially explained by the averaged relative changes in VIs. However, for the drought-affected regions, even when the average VIs did not change, GPP can still decline ~20% (intercept in Figures 1d–1f).

3.2 Sensitivity of GPP Anomalies to Changes in Vegetation Indices and Climate at 8 Day Intervals During the Drought Period

We calculated the partial correlations between GPP and VIs (with climate variables in control) or climate variables (with VIs in control) in both absolute and relative anomalies and investigated GPP responses to canopy and physiological controls. We chose EVI with different time lags to represent the canopy control and VPD with no lag for the physiological control because the anomalies of these predictors have higher correlations with GPP anomalies. There are clear differences between forest and nonforest ecosystems with respect to vegetation canopy versus physiological controls (Figure 2). All nonforest sites, while only about half of the forest sites, show strong partial correlation ($\rho > 0.5$) in relative anomalies ($\rho_\delta^{GPP,EVI}$, Figure 2c). The lags where the highest correlation is reached are also shorter for nonforest than forest sites. Strong partial correlation ($\rho > 0.5$) between GPP and VPD in absolute anomalies ($\rho_\Delta^{GPP,VPD}$) is found for most (seven out of nine) forest sites (Figure 2b). In contrast, $\rho_\Delta^{GPP,VPD}$ is positive for most nonforest sites. The correlations calculated using relative anomalies ($\rho_\delta^{GPP,VPD}$) are weaker than that using absolute anomalies ($\rho_\Delta^{GPP,VPD}$, Figure 2d). These analyses were also conducted for the two other VIs (NDVI and LSWI) with VPD and all three VIs with LST; the correlations become weaker when using LST instead of VPD (Figures S6–S10).
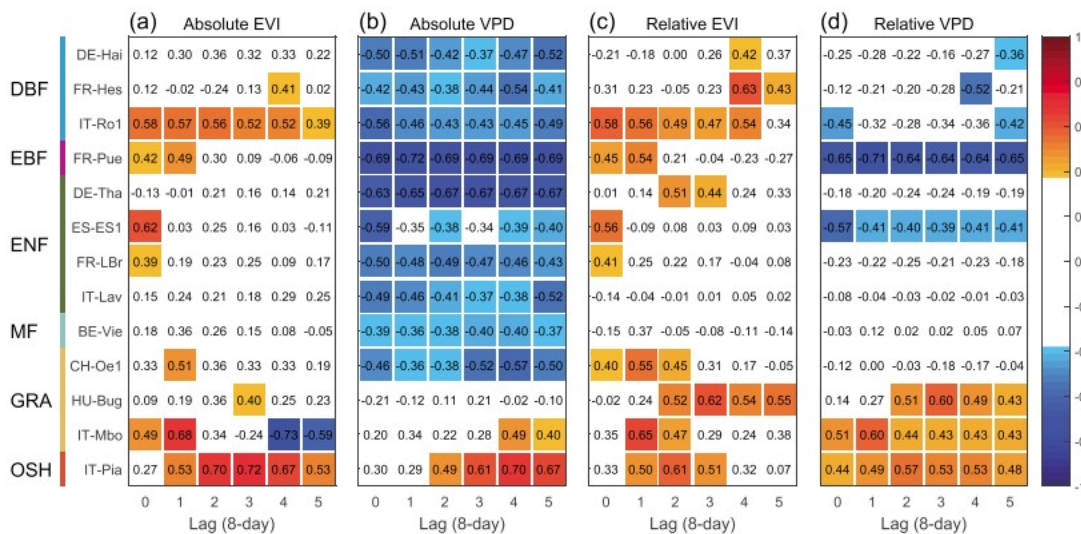

Figure 2. Partial correlation between anomalies in GPP and anomalies in (a and c) EVI and (b and d) VPD. EVI with different lags were used. Figures 2a and 2b are using absolute anomalies (Δ_γ) and Figures 2c and d2 are using relative anomalies (σ_γ). Only partial correlations that are significant at 0.1 level ($p < 0.1$) are shown in reddish or bluish color. The numbers represent the partial correlation coefficients.

We further use equations 4 and 5 to decompose the canopy and physiological controls, and the results are shown in Table 1. When using absolute anomalies (Δ), nonforest ecosystems usually have a higher level of significance for canopy sensitivity (Φ_{CC}) in the regression model, with an average value of $19.85 \pm 9.25\,g\,C\,m^{-2}\,d^{-1}/(EVI)$; forest ecosystems have a higher level of significance for physiological sensitivity (Φ_{PC}), with an average value of $-0.18 \pm 0.05\,g\,C\,m^{-2}\,d^{-1}/hPa$. When using the relative anomalies (δ), canopy sensitivity (φ_{CC}) shows a higher control of GPP for nonforest sites ($1.81 \pm 0.32\%GPP/\%EVI$), but the physiological sensitivity (φ_{PC}) has much lower p values for forest ecosystems. We also found that all sensitivities (Φ_{CC}, Φ_{PC}, φ_{CC}, and φ_{PC}) have a large range of variation for all ecosystems. Forest and nonforest ecosystems show a distinct difference ($p < 0.1$, student's t test) for three sensitivity factors except for Φ_{CC} (Figure S11). Canopy sensitivities (Φ_{CC} and φ_{CC}) are lower for forest than nonforest, while physiological sensitivities (Φ_{PC} and φ_{PC}) are opposite in absolute values. This regression analysis confirms the finding of the partial correlation analysis, and the results are similar when using different canopy indicators (NDVI and LSWI) and physiological indicator (LST) (Tables S2–S6).

Table 1. Parameters of the Regression Models for Both Absolute Anomalies (Δ) and Relative Anomalies (δ)[a]

| Site | IGBP Class | Absolute Anomaly (Δ) | | | | | | Relative Anomaly (δ) | | | | | |
		Φ_{CC}	p Value	Φ_{PC}	p Value	R^2	Lag	φ_{CC}	p Value	φ_{PC}	p Value	R^2	Lag
DE-Hai	DBF	11.70	0.127	−0.18	0.070	0.34	2	0.39	0.076	−0.05	0.264	0.22	4
FR-Hes	DBF	20.90	0.084	−0.23	0.017*	0.32	4	1.72	0.004**	−0.12	0.021*	0.42	4
IT-Ro1	DBF	18.02	0.010**	−0.15	0.012*	0.55	0	2.00	0.009**	−0.23	0.054	0.51	0
FR-Pue	EBF	19.93	0.032*	−0.20	0.001***	0.60	1	2.89	0.017*	−0.72	0.001***	0.58	1
DE-Tha	ENF	2.60	0.384	−0.24	0.002**	0.47	2	0.37	0.025*	−0.05	0.323	0.29	2
ES-ES1	ENF	17.61	0.005**	−0.24	0.008**	0.48	0	0.80	0.013*	−0.32	0.011*	0.43	0
FR-LBr	ENF	8.05	0.095	−0.15	0.029*	0.35	0	0.52	0.083	−0.06	0.333	0.21	0
IT-Lav	ENF	6.30	0.222	−0.12	0.106	0.33	4	0.07	0.825	0.00	0.966	0.00	4
BE-Vie	MF	6.56	0.134	−0.10	0.125	0.26	1	0.52	0.118	0.02	0.626	0.14	1
CH-Oe1	GRA	31.88	0.025*	−0.21	0.130	0.44	1	2.08	0.014*	0.00	0.992	0.31	1
HU-Bug	GRA	15.98	0.090	0.13	0.393	0.21	3	1.82	0.004**	0.54	0.006**	0.40	3
IT-Mbo	GRA	21.39	0.001***	0.12	0.150	0.50	1	1.36	0.003**	0.08	0.007**	0.56	1
IT-Pia	OSH	10.13	0.000***	0.10	0.005**	0.64	3	1.99	0.006**	0.45	0.010**	0.51	2

[a]Φ_{CC} and Φ_{PC} are the GPP sensitivity to absolute changes in canopy control and physiological control, respectively. φ_{CC} and φ_{PC} are the sensitivity of relative changes in canopy and physiological controls, respectively. p values are the significance of independent variables in the regressions. The lags are determined based on the strongest partial correlation between GPP anomalies and corresponding VIs. In this table, EVI is used to represent the canopy control and VPD is used to represent the physiological control. Entries in italics indicate positive sensitivity factors (Φ or φ).
*Indicates significance at 0.05 level.
**Indicates significance at 0.01 level.
***Indicates significance at 0.001 level.

4 Discussion

4.1 Differences Between Forest and Nonforest Ecosystems in Response to Drought and Heat Wave

Relative changes in GPP vary among biomes due to different resistance to drought. Forest ecosystems have deeper roots and higher regulatory capacity on transpiration during the early and middle phases of an extreme drought like 2003 [*Teuling et al.*, 2010]; therefore, they can better utilize soil water and are more resistant to short-term drought. Nonforest ecosystems are more vulnerable to drought due to their lower capability to utilize soil water [*Baldocchi et al.*, 2004]. The difference between forests and grasslands

is also supported by distinctive energy balance between forests and grasslands during the drought and heat wave period [*Teuling et al.*, 2010; *Wicke and Bernhofer*, 1996; *Zaitchik et al.*, 2006].

GPP anomaly is regulated by the combined effects of canopy and physiological changes. For forest ecosystems, the canopy changes are minor, and GPP anomalies primarily come from physiological limitation on photosynthesis. For nonforest ecosystems (GRA and OSH), both physiological and vegetation canopy changes contribute to the change in GPP during the drought and heat wave period. Canopy changes are dominant for these nonforest ecosystems, with previous studies showing that in situ measured LAI has a good correlation with GPP during the drought period [*Aires et al.*, 2008]. Although forest and nonforest ecosystems have different regulatory mechanisms, VIs can partially explain the observed relative changes in GPP during the drought across different biomes. By contrast, the physiological control (VPD or LST) on photosynthesis is a fast process and cannot be temporally averaged to evaluate the cross-site GPP differences during the entire drought period.

4.2 A Conceptual Model for Canopy and Physiological Limitations on Forest and Nonforest During Drought and Heat Wave

Indicators perform differently for temporally tracking the GPP anomalies at each site. In general, forest sites show weaker correlation between VI anomalies and GPP anomalies and have longer lags (but with large differences across sites), which makes it difficult to predict drought impacts on GPP using only VIs. GRA and OSH have shorter lags and show stronger correlation with VIs because of the higher SSWS. For forest ecosystems, VPD is a superior predictor of GPP anomalies over VIs. However, GPP responses to VPD may vary for different forest types and even for specific sites [*Lin et al.*, 2015]. Together with different VPD base values for the referential period, they contribute to the higher partial correlation when using absolute VPD anomalies rather than relative anomalies (Figure 2). Nonforest ecosystems have a lower sensitivity to VPD possibly because of less stomatal regulation and the relatively dominant role of vegetation canopy change in affecting GPP.

Based on the above findings, we built a conceptual model to describe the relationship among the relative anomalies in VPD, VIs, and GPP (Figure 3). The anomaly in GPP is the combined result of VPD and VI anomalies, with remarkable differences between forest and nonforest ecosystems. The drought can be divided into two periods: P-I is the initial period of drought, in which the VPD and radiation increases, but the canopy does not start to change due to the available soil water and ecosystem self-regulation. During this period, the primary regulation on GPP is through VPD and temperature. Forests have a much longer P-I, with higher sensitivity to VPD than nonforests. P-II starts when soil water is depleted and cannot sustain water supply to meet transpiration demand of plants, and the falling leaves result

in the changes in vegetation canopy or VIs. During this period, the primary regulation on GPP is the vegetation canopy. Nonforest ecosystems have a longer P-II phase than forests, and the VIs may change enormously during this period due to the senescence of leaves.
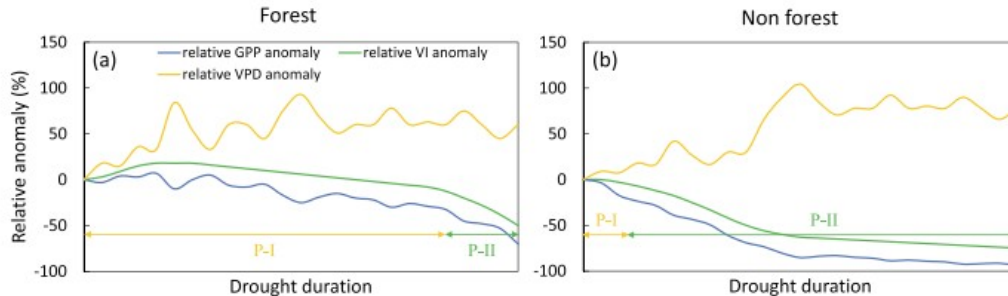

Figure 3. The conceptual model for vegetation canopy and physiological controls on (a) forest and (b) nonforest during the drought period. Relative anomalies (σ_y) were used. For simplicity and readability, VI fluctuation was removed, and only the VI trend was plotted. As drought progresses over time, two different drought stages are annotated as P-I and P-II. For the first stage (P-I), physiological control dominates the GPP variation, and for the second stage (P-II), canopy control dominates the GPP variation.

4.3 Implication and Limitation of the Canopy and Physiological Control Analyses

Different drought stages and regulation factors in forest and nonforest ecosystems suggest that we cannot use a single indicator to temporally track the GPP anomaly during the drought period for all ecosystems. For nonforest ecosystems, canopy control, which explains much of the GPP variation, has been partially embedded in the fraction of photosynthetic active radiation in PEMs (canopy sensitivity (φ_{CC}) is greater than 1%GPP/%EVI). The physiological control on GPP still exists but has much smaller variation. Because of the decoupling of atmospheric and soil water deficit from photosynthesis during extreme drought condition [*Beringer et al.*, 2011; *Yuan et al.*, 2014], VPD and other climate factors may not well represent physiological control on GPP at daily or longer time scales. Rapid canopy responses in nonforest ecosystems allow transformed VIs to be used to represent the physiological control on GPP, such as the LSWI-based water scalar used in VPM [*Xiao et al.*, 2004b]. For forest sites, VPD can be used, but more site-specific parameters are required. Similar biome-based differences were also reported by *Zhang et al*. [2015b]. Because the absolute anomaly of VPD (Δ_{VPD}) shows an advantage over the relative anomaly (δ_{VPD}) in both partial correlation analysis and the regression model (Figure 2 and Table 1), it also suggests a nonlinear response of VPD control on photosynthesis rather than the piecewise function currently used in MODIS PSN model [*Running et al.*, 2000].

The 2003 European drought and heat wave gives us a unique opportunity to study the drought impact on GPP and the feasibility of estimating the drought impacts on GPP using remote sensing-based PEMs. This research

benefits from high density of carbon flux towers; however, it also faces the following limitations:

The inconsistency of the flux tower footprint and MODIS pixel size; the land cover is relatively patchy and mixed pixels exist. The climate and GPP anomalies are also much larger in finer resolution images [*Zaitchik et al.*, 2006].

1. The data quality of VIs may still be unreliable even after gap filling and smoothing for some sites. This issue is more critical when doing interannual analysis at temporal scales but can be alleviated when VIs values are averaged over the entire drought period.

2. GPP and satellite-retrieved data are at 8 day time scale; however, VPD/ LST affects photosynthesis at the hourly scale; the inconsistency of operation time scales will also reduce the model predictability.

3. Several subsequent droughts and heat waves also influenced parts of Europe in 2006 and 2011. However, these years were not eliminated when calculating the reference values because of the different spatial extents and severities of these drought events.

5 Conclusions

This study presents an analysis of how GPP from different ecosystems responds to drought through vegetation canopy change and physiological responses. Distinctive responses to drought are found between forest and nonforest ecosystems. During the entire drought period, forests do not show obvious changes in canopy optical characteristics, while nonforests tend to have a faster canopy response. Relative anomalies of VIs can still be used as indicators to evaluate the drought-induced GPP decline spatially. At the temporal scale for each site, because of different dominant factors in two drought stages (P-I/P-II) and the different stage lengths for forest and nonforest, forest GPP is more responsive to changes in VPD, while nonforest GPP is more sensitive to changes in VIs. In the near future, soil moisture data from Soil Moisture Active Passive (SMAP) satellite and sun-induced chlorophyll fluorescence observations from Orbiting Carbon Observatory-2 (OCO-2) or Sentinel-5 Precursor satellite may be used to provide a better estimation of GPP decline from canopy and physiological controls during severe drought and heat wave period.

References

Aires, L. M. I., C. A. Pio, and J. S. Pereira (2008), Carbon dioxide exchange above a Mediterranean C3/C4 grassland during two climatologically contrasting years, *Global Change Biol.*, 14(3), 539– 555.

Allen, C. D., et al. (2010), A global overview of drought and heat-induced tree mortality reveals emerging climate change risks for forests, *For. Ecol. Manage.*, 259(4), 660– 684.

Anav, A., et al. (2015), Spatiotemporal patterns of terrestrial gross primary production: A review, *Rev. Geophys.*, 53, 785– 818, doi:10.1002/2015RG000483.

Arora, V. K., et al. (2013), Carbon-concentration and carbon-climate feedbacks in CMIP5 earth system models, *J. Clim.*, 26(15), 5289– 5314.

Baldocchi, D. D., L. K. Xu, and N. Kiang (2004), How plant functional-type, weather, seasonal drought, and soil physical properties alter water and energy fluxes of an oak-grass savanna and an annual grassland, *Agric. For. Meteorol.*, 123(1-2), 13– 39.

Beer, C., M. Reichstein, E. Tomelleri, P. Ciais, M. Jung, N. Carvalhais, C. Rödenbeck, M. A. Arain, D. Baldocchi, and G. B. Bonan (2010), Terrestrial gross carbon dioxide uptake: Global distribution and covariation with climate, *Science*, 329(5993), 834– 838.

Beringer, J., et al. (2011), Special-savanna patterns of energy and carbon integrated across the landscape, *Bull. Am. Meteorol. Soc.*, 92(11), 1467– 1485.

Blackman, C. J., and T. J. Brodribb (2009), Leaf hydraulics and drought stress: Response, recovery and survivorship in four woody temperate plant species, *Plant, Cell Environ.*, 32(11), 1584– 1595.

Carlson, T. N., and D. A. Ripley (1997), On the relation between NDVI, fractional vegetation cover, and leaf area index, *Remote Sens. Environ.*, 62(3), 241– 252.

Ciais, P., M. Reichstein, N. Viovy, A. Granier, J. Ogée, V. Allard, M. Aubinet, N. Buchmann, C. Bernhofer, and A. Carrara (2005), Europe-wide reduction in primary productivity caused by the heat and drought in 2003, *Nature*, 437(7058), 529– 533.

Dai, A. (2012), Increasing drought under global warming in observations and models, *Nat. Clim. Change*, 3(1), 52– 58.

der Molen, V. M. K., A. J. Dolman, P. Ciais, and T. Eglin (2011), Drought and ecosystem carbon cycling, *Agric. For. Meteorol.*, 151(7), 765– 773.

Dong, J., et al. (2015), Comparison of four EVI-based models for estimating gross primary production of maize and soybean croplands and tallgrass prairie under severe drought, *Remote Sens. Environ.*, 162, 154– 168.

Easterling, D. R., G. A. Meehl, C. Parmesan, S. A. Changnon, T. R. Karl, and L. O. Mearns (2000), Climate extremes: Observations, modeling, and impacts, *Science*, 289(5487), 2068– 2074.

Farquhar, G. D., S. V. Caemmerer, and J. A. Berry (1980), A biochemical-model of photosynthetic CO_2 assimilation in leaves of C-3 species, *Planta*, 149(1), 78– 90.

Flexas, J., and H. Medrano (2002), Drought-inhibition of photosynthesis in C3 plants: Stomatal and non-stomatal limitations revisited, *Ann. Bot.*, 89(2), 183– 189.

Frank, D., et al. (2015), Effects of climate extremes on the terrestrial carbon cycle: Concepts, processes and potential future impacts, *Global Change Biol.*, 21, 2861– 2880, doi:10.1111/gcb.12916.

Hetherington, A. M., and F. I. Woodward (2003), The role of stomata in sensing and driving environmental change, *Nature*, 424(6951), 901– 908.

Ji, L., and A. J. Peters (2003), Assessing vegetation response to drought in the northern Great Plains using vegetation and drought indices, *Remote Sens. Environ.*, 87(1), 85– 98.

Jung, M., et al. (2011), Global patterns of land-atmosphere fluxes of carbon dioxide, latent heat, and sensible heat derived from eddy covariance, satellite, and meteorological observations, *J. Geophys. Res.*, 116, G00J07, doi:10.1029/2010JG001566.

Lin, Y.-S., et al. (2015), Optimal stomatal behaviour around the world, *Nat. Clim. Change*, 5, 459– 464, doi:10.1038/nclimate2550.

Liu, J., S. Rambal, and F. Mouillot (2015), Soil drought anomalies in MODIS GPP of a Mediterranean broadleaved evergreen forest, *Remote Sens.*, 7(1), 1154– 1180.

Mahadevan, P., S. C. Wofsy, D. M. Matross, X. M. Xiao, A. L. Dunn, J. C. Lin, C. Gerbig, J. W. Munger, V. Y. Chow, and E. W. Gottlieb (2008), A satellite-based biosphere parameterization for net ecosystem CO_2 exchange: Vegetation Photosynthesis and Respiration Model (VPRM), *Global Biogeochem. Cycles*, 22, GB2005, doi:10.1029/2006GB002735.

Peng, C. H., Z. H. Ma, X. D. Lei, Q. Zhu, H. Chen, W. F. Wang, S. R. Liu, W. Z. Li, X. Q. Fang, and X. L. Zhou (2011), A drought-induced pervasive increase in tree mortality across Canada's boreal forests, *Nat. Clim. Change*, 1(9), 467– 471.

Reichstein, M., J. D. Tenhunen, O. Roupsard, J. M. Ourcival, S. Rambal, F. Miglietta, A. Peressotti, M. Pecchiari, G. Tirone, and R. Valentini (2002), Severe drought effects on ecosystem $CO(2)$ and $H(2)O$ fluxes at three

Mediterranean evergreen sites: Revision of current hypotheses? *Global Change Biol.*, 8(10), 999– 1017.

Running, S. W., P. E. Thornton, R. Nemani, and J. M. Glassy (2000), Global terrestrial gross and net primary productivity from the earth observing system, in *Methods in Ecosystem Science*, edited by O. E. Sala et al., pp. 44– 57, Springer, New York.

Running, S. W., R. R. Nemani, F. A. Heinsch, M. S. Zhao, M. Reeves, and H. Hashimoto (2004), A continuous satellite-derived measure of global terrestrial primary production, *BioScience*, 54(6), 547– 560.

Saatchi, S., S. Asefi-Najafabady, Y. Malhi, L. E. O. C. Aragao, L. O. Anderson, R. B. Myneni, and R. Nemani (2013), Persistent effects of a severe drought on Amazonian forest canopy, *Proc. Natl. Acad. Sci. U.S.A.*, 110(2), 565– 570.

Schaefer, K., et al. (2012), A model-data comparison of gross primary productivity: Results from the North American Carbon Program site synthesis, *J. Geophys. Res.*, 117, G03010, doi:10.1029/2012JG001960.

Schar, C., P. L. Vidale, D. Luthi, C. Frei, C. Haberli, M. A. Liniger, and C. Appenzeller (2004), The role of increasing temperature variability in European summer heatwaves, *Nature*, 427(6972), 332– 336.

Sims, D. A., E. R. Brzostek, A. F. Rahman, D. Dragoni, and R. P. Phillips (2014), An improved approach for remotely sensing water stress impacts on forest C uptake, *Global Change Biol.*, 20(9), 2856– 2866.

Sitch, S., et al. (2008), Evaluation of the terrestrial carbon cycle, future plant geography and climate-carbon cycle feedbacks using five Dynamic Global Vegetation Models (DGVMs), *Global Change Biol.*, 14(9), 2015– 2039.

Teuling, A. J., S. I. Seneviratne, R. Stöckli, and M. Reichstein (2010), Contrasting response of European forest and grassland energy exchange to heatwaves, *Nat. Geosci.*, 3(10), 722– 727.

Turner, D. P., W. D. Ritts, J. M. Styles, Z. Yang, and W. B. Cohen (2006), A diagnostic carbon flux model to monitor the effects of disturbance and interannual variation in climate on regional NEP, *Tellus B*, 58(5), 476– 490.

Vetter, M., et al. (2008), Analyzing the causes and spatial pattern of the European 2003 carbon flux anomaly using seven models, *Biogeosciences*, 5(2), 561– 583.

Wan, Z., P. Wang, and X. Li (2004), Using MODIS land surface temperature and normalized difference vegetation index products for monitoring drought in the southern Great Plains, USA, *Int. J. Remote Sens.*, 25(1), 61– 72.

Wicke, W., and C. Bernhofer (1996), Energy balance comparison of the Hartheim forest and an adjacent grassland site during the HartX experiment, *Theor. Appl. Climatol.*, 53(1-3), 49– 58.

Xiao, X. M., Q. Y. Zhang, D. Hollinger, J. Aber, and B. Moore (2005), Modeling gross primary production of an evergreen needleleaf forest using MODIS and climate data, *Ecol. Appl.*, 15(3), 954– 969.

Xiao, X., D. Hollinger, J. Aber, M. Goltz, E. A. Davidson, Q. Zhang, and B. Moore (2004a), Satellite-based modeling of gross primary production in an evergreen needleleaf forest, *Remote Sens. Environ.*, 89(4), 519– 534.

Xiao, X., Q. Zhang, B. Braswell, S. Urbanski, S. Boles, S. Wofsy, B. Moore, and D. Ojima (2004b), Modeling gross primary production of temperate deciduous broadleaf forest using satellite images and climate data, *Remote Sens. Environ.*, 91(2), 256– 270.

Yuan, W., et al. (2014), Global comparison of light use efficiency models for simulating terrestrial vegetation gross primary production based on the LaThuile database, *Agric. For. Meteorol.*, 192-193, 108– 120.

Zaitchik, B. F., A. K. Macalady, L. R. Bonneau, and R. B. Smith (2006), Europe's 2003 heat wave: A satellite view of impacts and land-atmosphere feedbacks, *Int. J. Climatol.*, 26(6), 743– 769.

Zhang, Q., X. Xiao, B. Braswell, E. Linder, F. Baret, and B. Mooreiii (2005), Estimating light absorption by chlorophyll, leaf and canopy in a deciduous broadleaf forest using MODIS data and a radiative transfer model, *Remote Sens. Environ.*, 99(3), 357– 371.

Zhang, Y., C. Peng, W. Li, X. Fang, T. Zhang, Q. Zhu, H. Chen, and P. Zhao (2013), Monitoring and estimating drought-induced impacts on forest structure, growth, function, and ecosystem services using remote-sensing data: Recent progress and future challenges, *Environ. Rev.*, 21(2), 103– 115.

Zhang, Y., W. Z. Li, Q. Zhu, H. Chen, X. Q. Fang, T. L. Zhang, P. X. Zhao, and C. H. Peng (2015a), Monitoring the impact of aerosol contamination on the drought-induced decline of gross primary productivity, *Int. J. Appl. Earth Obs. Geoinf.*, 36, 30– 40.

Zhang, Y., C. Song, G. Sun, L. E. Band, A. Noormets, and Q. Zhang (2015b), Understanding moisture stress on light use efficiency across terrestrial ecosystems based on global flux and remote-sensing data, *J. Geophys. Res. Biogeosci.*, 120, 2053– 2066, doi:10.1002/2015JG003023.

Zhao, M., and S. W. Running (2010), Drought-induced reduction in global terrestrial net primary production from 2000 through 2009, *Science*, 329(5994), 940– 943.

Zscheischler, J., M. Reichstein, S. Harmeling, A. Rammig, E. Tomelleri, and M. D. Mahecha (2014), Extreme events in gross primary production: A characterization across continents, *Biogeosciences*, 11(11), 2909– 2924.